Simulation-Based Engineering Lab
University of Wisconsin-Madison

Technical Report TR-2020-05

Drawbar Pull Testing of Autonomous Vehicle

Zach Gasick

August 8, 2020

Abstract

The Danish development company AgroIntelli has recently released the Robotti - an autonomous farming vehicle. As the Robotti is a new product, testing and development is ongoing. One experiment that is desired to be run is a drawbar pull test. To support the design of this experiment, a model was created using Project Chrono to determine the expected forces and torques in the coming experiment.

While the overall trends (such as increasing drawbar pull force over slip to a maximum value, or increasing wheel torque with drawbar pull force) that occur in real life tests were confirmed by the simulations, there were some unexpected results. One of the rear tires was observed to sink a large amount compared to the other three tires. This is believed to be caused by a combination of vehicle asymmetry, soil stiffness and soil erosion.

Contents

1 Introduction

AgroIntelli, a Danish development company in the farming industry, has recently created an autonomous farming vehicle called the Robotti. The Robotti is capable of performing multiple tasks such as precision planting, weeding, and seed drilling. As this is a new product, testing and development is ongoing. One test that is desired to be run is a drawbar pull experiment. This experiment was simulated to give the engineers a better idea of what forces would be expected in order to better design and calibrate their experiment.

When the engineers run the drawbar pull test, they will hook up the Robotti to a heavier follower vehicle moving at a fixed velocity. The Robotti will attempt to move at a faster velocity, inducing slip in the wheels. This scenario was modelled in Project Chrono. The force exerted by the follower vehicle was then analyzed, along with the wheel torques necessary to run the Robotti.

2 Model Formulation

The model itself can be viewed in three distinct parts: the Robotti itself, the drawbar rig, and the soil. There were a total of 13 bodies and 15 constraints including motors/drivers. In the simulation, the Robotti was allowed to achieve steady-state by including a three second buffer prior data collection. At the start of the simulation, the Robotti was dropped on to the soil, necessitating time for the wheels to return to nominal conditions. In drawbar pull tests in reality, the vehicle would be wheeled in to place as the tests begin. A buffer of three seconds was chosen based on several runs. This allowed the Robotti to clear the craters where the wheels had initially been dropped.

The simulation was set up to run as follows:

1. Initialize the model
   (a) create Robotti, drawbar rig, and soil
   (b) follower speed is set to 3 [km/hr]
   (c) wheel speed is set to 1/5 target speed
2. For 2 seconds, ramp up the wheel speed to the target speed
3. From 2 to 3 seconds, let the Robotti stabilize and reach steady state
4. From 3 to 4.5 seconds, gather desired data

2.1 Robotti Configuration

The Robotti contains 12 bodies, 7 constraints, and 4 motors, outlined in the following images.

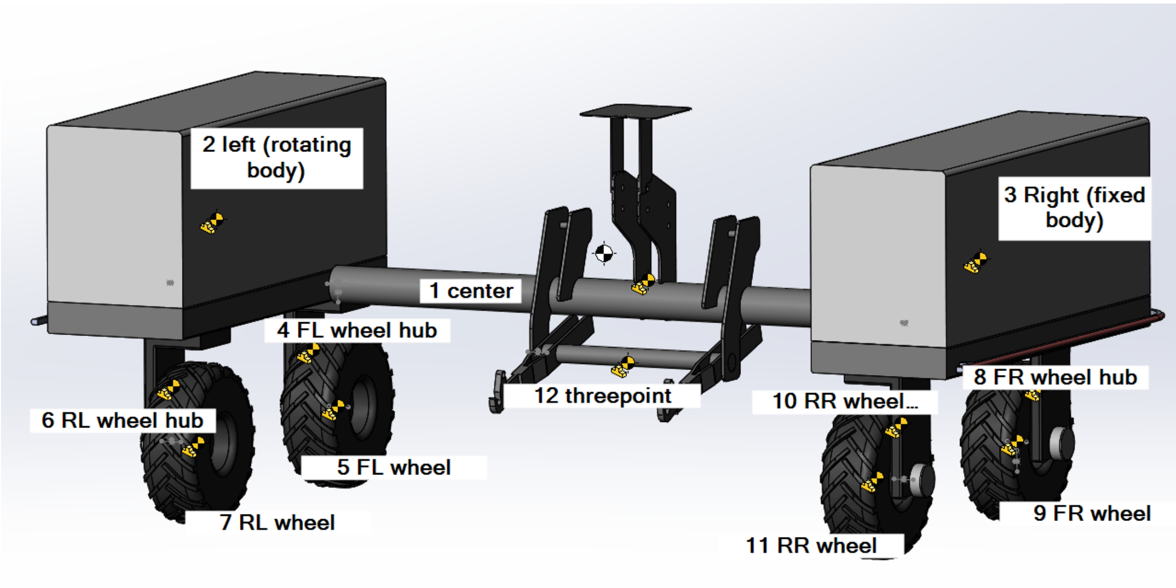

(a) Image of Bodies

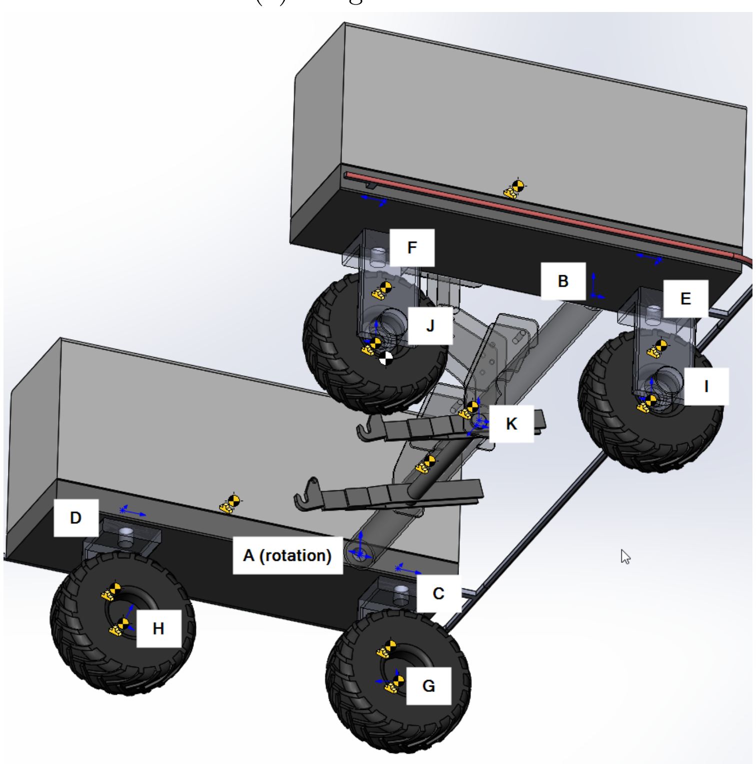

(b) Image of Constraints

Figure 1: Naming convention of bodies (a) and constraints (b)

Constraint Letter	Constraint Type	IDs of Bodies Joined	Translation DOF Fixed	Rotational DOF Fixed
A	Revolute	1, 2	3	2
B	Fixed	1, 3	3	3
C	Fixed	2, 4	3	3
D	Fixed	2, 6	3	3
E	Fixed	3, 8	3	3
F	Fixed	3, 10	3	3
G	Angular Speed Motor	4, 5	3	3*
H	Angular Speed Motor	6, 7	3	3*
I	Angular Speed Motor	8, 9	3	3*
J	Angular Speed Motor	10, 11	3	3*
K	Fixed	12, 1	3	3

Table 1: Constraint List.
*Kinematic constraint on 1 rotational degree of freedom

The Robotti has a few peculiarities in its design, namely that the vehicle is asymmetric laterally, and that the motors for the wheels connect directly to the wheels themselves. The motors control the vehicle speed by receiving a request from the the Robotti for a certain speed, then varying the output torque to yield the correct speed. The asymmetry of the vehicle can be seen in the use of a fixed constraint (joint ID B) between the right body (body ID 3) and the center bar (body ID 1), and a revolute joint (joint ID A) between the left body (body ID 2) and the center bar (body ID 1). The way the motors are implemented, they fix all degrees of freedom except the one that they are driving. In effect, they act like a revolute joint, with an additional kinematic constraint governing the rotation of the wheels.

The motors on the wheels were set up to build up to the desired speed over two seconds, allowing for stabilization between the various constraints so that consistent conditions would be met by the time data started to be acquired at three seconds. When the simulation begins, the Robotti is forced along at the follower vehicle's prescribed pace. The wheel speeds starts at one-fifth full speed and ramps up over the two seconds to the desired speed.

2.2 Drawbar Rig Configuration

The drawbar rig consists of 2 additional bodies with 3 constraints and a motor. One of the bodies is fixed in place, representing the ground, while the other is an intermediate body, allowing for more degrees of freedom in the Robotti. The intermediate body does not contribute anything else to the model, only allowing for additional degrees of freedom. Connecting the ground to the intermediate body is a prismatic constraint, which locks all motion and rotations, except for longitudinal translation (5 DOF fixed). A motor was inserted as well, applying a kinematic constraint between the ground and the intermediate body. The effect of this is that the intermediate body moves at a prescribed velocity - the follower vehicle's velocity, only moving in the longitudinal direction. For these experiments, the prescribed follower velocity was set to be 3 [km/hr].

The intermediate body was connected to the three point harness with a point-line constraint and a parallel constraint. The point-line constraint locked lateral and longitudinal DOFs, while allowing full rotation. This constraint, combined with the prismatic joint between the intermediate body and the ground, allowed the Robotti to move vertically and longitudinally at the follower vehicle's pace (due to the motor). The parallel constraint worked in tandem with the prismatic constraint to allow for pitching in the Robotti. To summarize, the drawbar rig prescribes longitudinal motion, while allowing vertical motion and pitching.

One issue faced in the model set up was the tendency for the Robotti to pitch on to its back at the higher wheel speeds. This is significant as it required two measures to be taken to prevent this behavior. The first measure consisted of reducing the motor speed at the instant of wheel-soil contact. Rather than initiating the motor to run at its final desired speed, the motor speed was ramped up to achieve this speed over time. When this is done, the front wheels tend to dig into the soil bed, preventing the pitching action and slowly driving the wheel speed up to the desired speed. This avoids the scenario where the vehicle goes from no traction as it is dropped on to the soil bed to full traction when the vehicle makes contact with the soil.

Due to unexpected results (discussed below), another model was created without any of the drawbar rig components. This was done to ensure that the vehicle on its own behaved as expected.

2.3 Terrain Configuration

The terrain the Robotti drove over was an adaptive mesh utilizing a combination of the Bekker-Wong soil model and the Janosi-Hanamoto shear model [1]. The soil contact model (SCM) consists of nodes that the tire meshes can come in contact with. If contact is detected on a node, the mesh around that node is refined. The nodes in contact are allowed to displace in the vertical direction only, with largely plastic deformations. Key parameters used in the SCM are highlighted below [1].

Parameter	Sandy Soil Value	Clayley Soil Value
Kphi (frictional modulus in Bekker model)	500000	814000
Kc (cohesive modulus in Bekker model)	3000	20680
n (exponent of sinkage in Bekker model)	1.1	1.0
Cohesion for shear failure	0	3500
Friction angle (degrees) for shear failure	30	11
J (shear parameter in Janosi-Hanamoto formula)	.01	.025
K (elastic stiffness per unit area)	$4{\cdot}10^7$	$7.8{\cdot}10^7$
R (vertical damping per unit area)	$3{\cdot}10^4$	$3{\cdot}10^4$

Table 2: Soil Parameters

The model was set to account for bulldozing as well. Parameters listed below.

Parameter	Value
Angle of erosion of the displaced material (degrees)	55
Growth of lateral volume respect to pressed volume	1
Number of erosion refinements per timestep	5
Number of concentric vertex selections subject to erosion	10

Table 3: Bulldozing Parameters

3 Results

When running the simulations, an unexpected trend emerged. The rear left tire on the revolute joint side of the model dug in to the soil more than that of the rear right tire (fixed joint side). The drawbar rig was removed to ensure that under nominal operating conditions and the Robotti behaved as expected.

3.1 Free Moving Robotti

In the first simulation, the Robotti was run on both soil types without any constraints from the drawbar rig. Below are the normal forces on the wheels as well as torque/speed curves. For the speed, based on how the wheel motors were modelled, the wheels' angular speed will not be the vehicle's speed if any slip is present. Thus, the angular speeds of the wheels are displayed. Assuming no slip, the angular speeds correspond to a Robotti velocity of three to seven [km/hr]. Both soils were tested, with the results shown below, with the sandy soil results on the left and the Clayley soil model on the right.

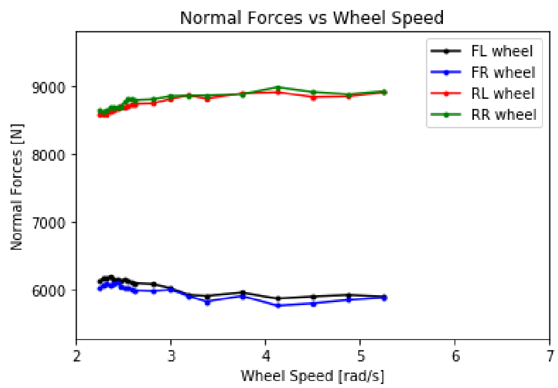

(a) Normal Forces vs Wheel Speed for Sandy Soil

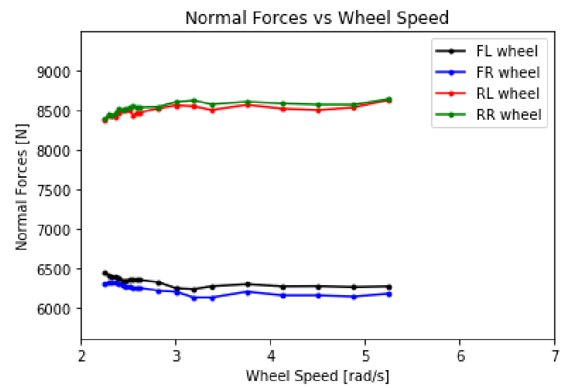

(b) Normal Forces vs Wheel Speed for Clayley Soil

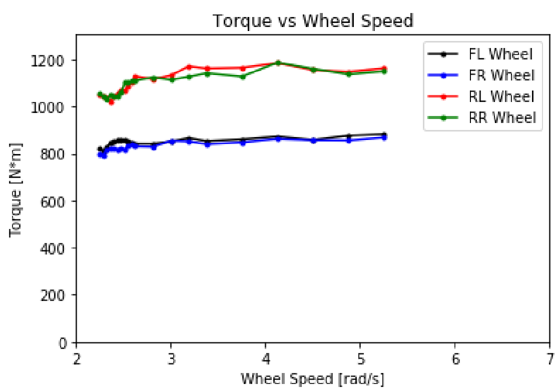

(c) Torque to Maintain Wheel Speed for Sandy Soil

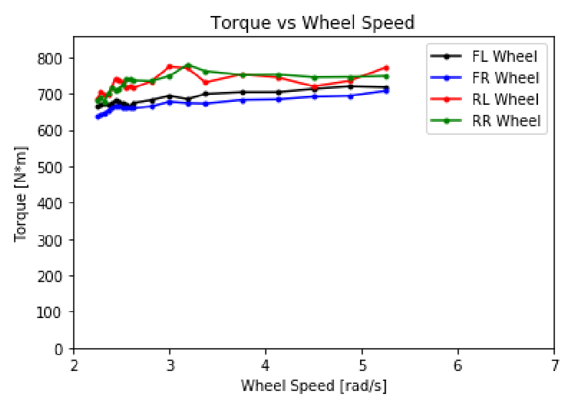

(d) Torque to Maintain Wheel Speed for Clayley Soil

Figure 2: Results for Free Moving Robotti

Regarding the normal forces, it is clear that the center of mass sits towards the rear of the vehicle. In the simulations, there is a slight tendency for the vehicle to pitch, as can be seen by small increases to the normal forces on the rear tires and small decreases to the normal forces on the front tires.

With the plots of the torques, there is a large increase in the torque to run the Robotti in the softer sandy soil as opposed to the more rigid Clayley soil. This aligned with expectations, as with the softer soil came more sinkage, leading to the increased torque requirements.

3.2 Drawbar Pull Test

In the drawbar pull simulations, the rear left tire sinkage lead to large differences in the rear right vs rear left torque outputs. This occured to a greater degree at higher slips.

For the torqe and drawbar pull force graphs, slip was calculated and plotted as the x axis. Wheel slip was defined using:

$$S = 1 - \frac{V}{r\ \omega} \tag{1}$$

where S is the wheel slip, V is the linear vehicle velocity, r is the tire radius, and ω is the angular velocity of the tire.

Below, wheel torques, normal forces, and the drawbar pull force are plotted against slips or wheel speeds. As before, the sandy soil results are on the left and the Clayley soil is on the right.

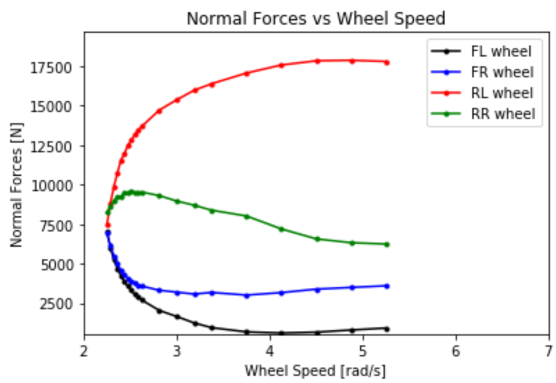

(a) Normal Forces vs Wheel Speed for Sandy Soil

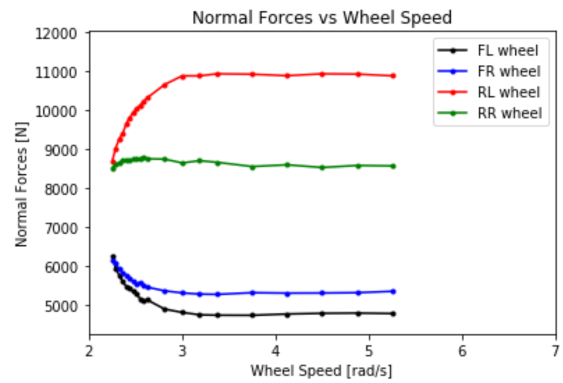

(b) Normal Forces vs Wheel Speed for Clayley Soil

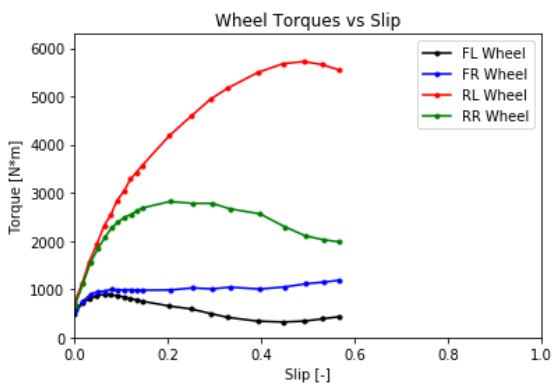

(c) Torque to Maintain Slip for Sandy Soil

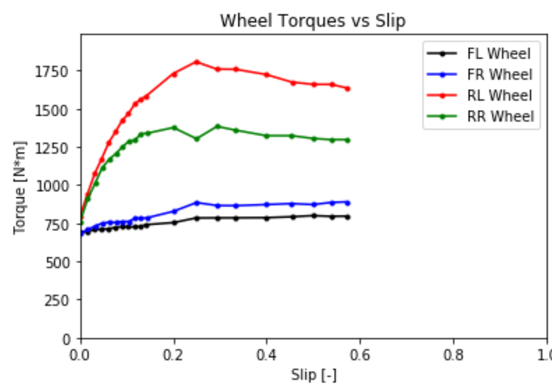

(d) Torque to Maintain Slip for Clayley Soil

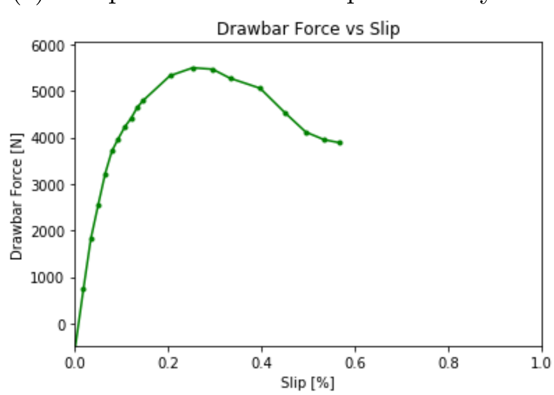

(e) Drawbar Pull Force vs Wheel Slip for Sandy Soil

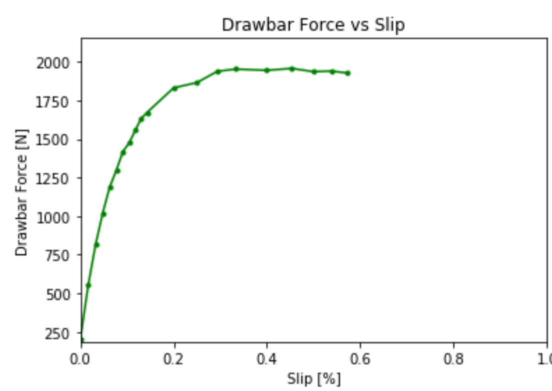

(f) Drawbar Pull Force vs Wheel Slip for Clayley Soil

Figure 3: Drawbar Pull Simulation Results

Initially, the results from the drawbar pull tests appear unexpected. However, when several factors are accounted for, the results become reasonable.

The first key to understanding the results is in recalling that the Robotti is asymmetric. The two main body components (body ID's 2 and 3) are attached to the center bar (body ID 1) via a revolute joint and a weld, respectively. This indicates symmetry in the data should not be expected when reviewing the results of the simulation. Additionally, the center of mass is towards the rear of the Robotti, meaning that in addition to lateral asymmetry, there is also longitudinal asymmetry.

The second phenomenon is the sinkage of the rear left tire, as seen below.

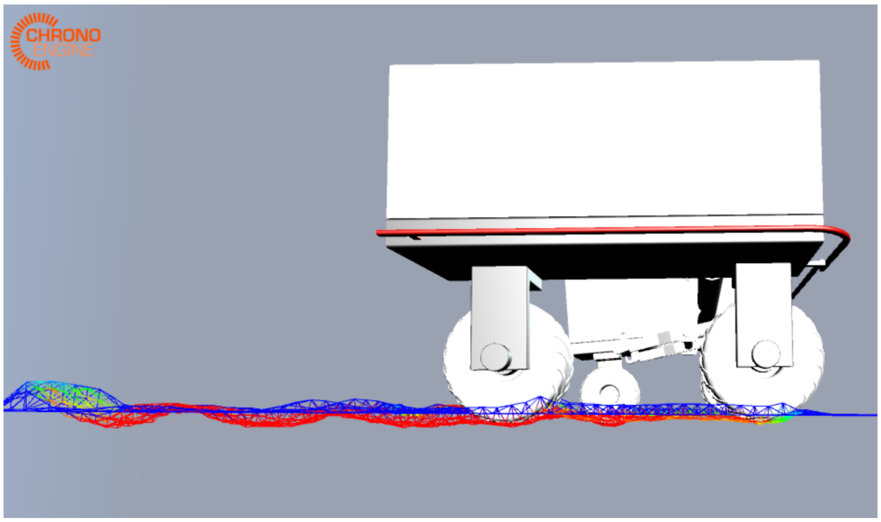

(a) Vehicle Right Side Sinkage (moving to the right)

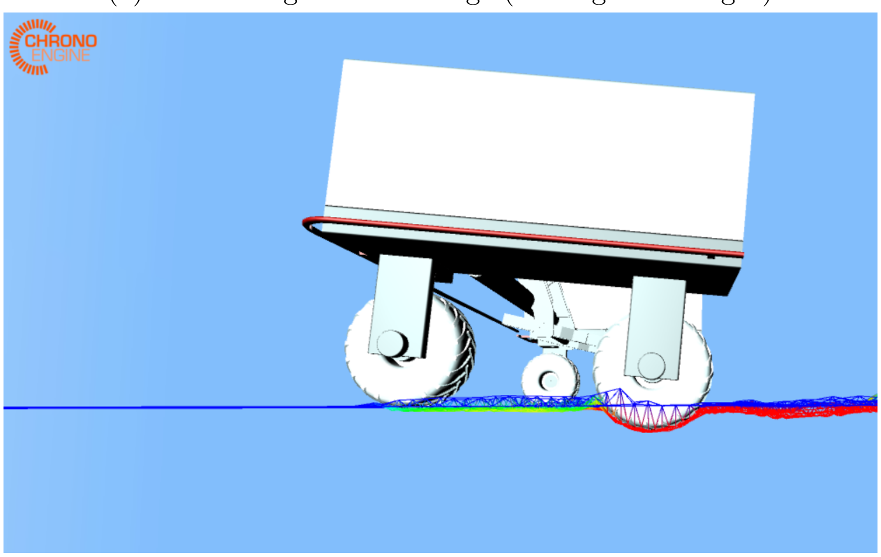

(b) Vehicle Left Side Sinkage (moving to the left)

Figure 4: Side view of the Robotti during simulation

Several tests were performed to confirm the validity of the results, one of which was simply switching the location of the revolute and fixed joints. When this was done, the results were identical, except mirrored left to right. This eliminates the possibility of an incorrect configuration of the motors or other constraints. Another test was to use two welds instead of a revolute joint and a weld. This led to symmetric results, leading to the conclusion that the sinkage of the rear left tire is an accurate phenomenon.

Understanding these details, the normal forces plot behaves largely as expected. At higher speeds, the rear left tire sinks further into the soil, causing a higher normal force. This in turn lifts the front left tire, leading to normal forces. This is also compounded by a net moment acting on the vehicle between the drawbar pull force pulling the vehicle backwards and the traction from the tires pushing the vehicle forwards. This is seen in the pitching of the vehicle. The net moment on the vehicle can be seen in the discrepancy between the front and rear tires' normal forces on the right hand side as well.

These effects are less prevalent in the stiffer soil. The phenomenon is still present, albeit at a lower magnitude, as indicated by the data in figure three.

The wheel torques for both soil models line up reasonably well with the normal forces, as the normal forces are a good indicator of the sinkage. When the tire sinks more, there is a larger amount of soil the tire is in contact with, and in addition to requiring torque to move the Robotti forward, torque is needed to try to pull the Robotti out of the run, leading to the larger torques corresponding to the higher normal forces. This lines up with the model's handling of soil erosion (Table 3 - Bulldozing Parameters) - the deeper the rut, the more the soil will erode, requiring more torque to overcome the motion from the soil erosion.

For the drawbar forces, the difference between the two soils comes back to the sinking of the tires. In the softer sandy soil, more sinkage occurs, leading to a larger amount of soil that the tire is in contact with. This leads to the development of larger traction. The reason for the dip in the sandy soil may be due to the erosion of the soil. At higher speeds, there will be a deeper rut. This in turn will lead to soil erosion, which facilitates slip in the wheel, meaning that less torque can be developed. In essence, there is an ideal amount of sinkage for maximizing the drawbar pull force. This sinkage is dependent on not only the soil (seen in the comparison between the graphs of the sandy soil and Clayley soil), but also on the slip (seen in particular on the sandy soil graph).

4 Future Work

The drawbar simulations provided good insight into what the Robotti would face in a drawbar pull test in the field, as the results indicate a correct order of magnitude when compared to the expected torque capacity of the motors in the field. However, this simulation was done with estimates for soil parameters. To improve the simulation, soil parameters from the field test location could be incorporated into the simulation.

Another area of concern is the motor models. The model was simplified to an angular speed kinematic constraint. Adding in controllers would allow for more realistic behavior of the motors and the torques they output.

5 Bibliography

[1] Tasora, A., Mangoni, D., Negrut, D., Serban, R. and Jayakumar, P. (2019) Deformable soil with adaptive level of detail for tracked and wheeled vehicles, *Int. J. Vehicle Performance*, Vol. 5, No. 1, pp.6076